Organic & Biomolecular Chemistry

Accepted Manuscript

ROYAL SOCIETY OF CHEMISTRY

www.rsc.org/obc

Journal Name

RSCPublishing

ARTICLE

A Fluorescent Turn-on H_2S-responsive Probe: Design, Synthesis and Application

Cite this: DOI: 10.1039/x0xx00000x

Yufeng Zhang,[1a] Haiyan Chen,[1b*] Dan Chen,[b] Di Wu,[a] Xiaoqiang Chen,[c] Sheng Hua Liu*[a] and Jun Yin*[a]

Received 00th January 2012,
Accepted 00th January 2012

DOI: 10.1039/x0xx00000x

www.rsc.org/

Hydrogen sulfide (H_2S) is considered as the third signaling molecule in vivo and it plays an important role in various physiological processes and pathological processes in vivo, such as vasodilation, apoptosis, neurotransmission, ischemia/reperfusion-induced injury, insulin secretion and inflammation. Developing a highly selective and sensitive method that can detect H_2S in biological system is very important. In this work, a colorimetric and "turn-on" fluorescent probe is developed. Furthermore, this probe displays a highly selective response to H_2S in aqueous solution and possesses a good capability for bioimaging H_2S without interferences in living cells. The results suggest that H_2S-selective probe has good water-solubility, biocompatibility and cell-penetrability and can be served as an efficient tool for probing H_2S in cell level.

Introduction

Hydrogen sulfide is considered as the third signaling molecule in vivo as well as nitric oxide and carbon monoxide.[1] Endogenous H_2S is primarily produced with the catalysis by enzymes such as cystathionine b-synthetase (CBS), cystathionine c-lyase (CSE) and 3-mercaptopyruvate sulphurtransferase (3-MST).[2] On the one hand, H_2S plays some important roles in various physiological processes and pathological processes in vivo, such as vasodilation, apoptosis, neurotransmission, ischemia/reperfusion-induced injury, insulin secretion and inflammation.[3] On the other hand, as a poisonous gas with rotten egg smell, high concentrations of H_2S can also harm the human body, showed symptoms of central nervous system and suffocation, and even lead to death.[4] Therefore, developing a highly selective and sensitive method that can detect H_2S and be applied in biological system is very significant.

Traditional methods such as gas chromatography, electrochemical analysis, colorimetric method, metal-induced sulfide precipitation have been applied in the detection of H_2S.[5] However, these methods usually suffer from the limitation in that they can only be used to detect H_2S in vitro. As mentioned above, H_2S as the signaling molecule in biosome participates in many biological functions. Therefore, developing the efficient approach suitable for the detection in microenvironment such as living cells is very significant. Due to its simplicity, high sensitivity and high selectivity, fluorescent probe technology has become an effective tool in the detection of intracellular H_2S in recent years,[6] Numerous H_2S-responsive fluorescent probes based on different mechanisms have been widely developed, including redox reaction, nucleophilicity cyclization, and metal sulfide formation.[6, 7]

In the field of environmental sensitive bioimaging, the turn-off fluorescent probes usually involve in some confusion especially for those interferences such as the environment, probe activity, biocompatibility, cellular penetration etc also result in the fluorescence quenching, except for the detected species.[8] While a turn-on fluorescent probe can overcome these disadvantage. As described above, many H_2S-responsive fluorescent probes have been reported, but the same trouble also exists in the design of H_2S probes.[6, 9] Herein, we present an efficient strategy for designing the turn-on fluorescent probes, in which a H_2S-responsive fluorescent probe is designed and applied for the detection of H_2S in living cells.

Results and discussion

Design and synthesis

Over the past years, the mechanism of nucleophilic reaction has been commonly used to design the H_2S probes owing to its strong nucleophilic reactivity.[10] Whether the probe is turn-on after treating with H_2S depends on the fluorescent emission of cleavage product. If the cleavage product is fluorescent, this probe would be a turn-on fluorescent probe. Accordingly, we propose this design strategy of turn-on fluorescent probe, as presented in Figure 1. In which, a fluorescent compound **A** is employed as a cleavage product to react with compound **B**, affording a non-fluorescent or weak fluorescent probe **A-B**. Upon the treatment of H_2S, the nucleophilic substituted reaction takes place, generating the corresponding nucleophilic substitution product **B-SH** and the cleavage product **A**. For fluorescent backbone **A**, it plays dual roles of cleavage product and leaving group while moiety **B** is required to be an electron-deficient system for meeting the needs of nucleophilic substituted reaction.

In previous work,[11] we found that dansylpiperazine (**DP**) is a fluorescent moiety with the fluorescence peak at 552 nm under the excitation with 330 nm. In this work, compound **DP** can be

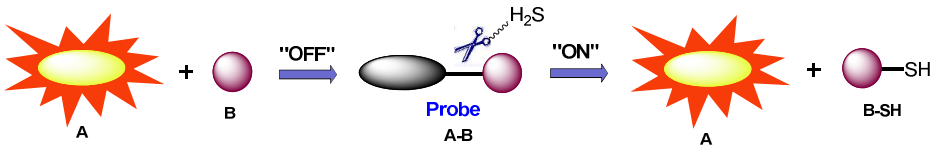

Figure 1 Designing principle of the turn-on H_2S-responsive fluorescent probes

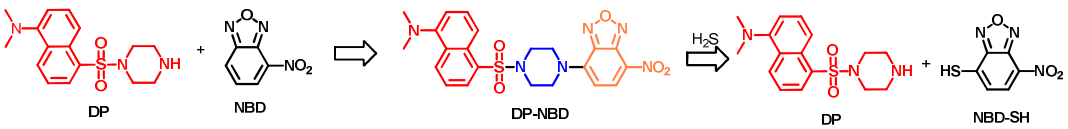

Scheme 1 Structure of the H_2S-responsive turn-on fluorescent probe **DP-NBD**

employed to serve as a cleavage product while nitrobenzo[c][1,2,5]oxadiazole (**NBD**) possesses strong electron-deficient feature. Therefore, two components compose the probe **DP-NBD**, as described in Scheme 1. Upon the attack of H_2S, the nucleophilic substituted reaction will take place, affording the corresponding product **NBD-SH** and the fluorescent cleavage product **DP**. This design will guarantee that **DP-NBD** is a fluorescence turn-on probe for H_2S.

According to the strategy described in Scheme 1, the probe **DP-NBD** can be synthesized according to the two different synthetic routes outlined in Scheme 2. One strategy is described in Scheme 2(A). The intermediate **DP**, prepared by the reaction of dansyl chloride with piperazine, is treated with 4-chloro-7-nitrobenzofurazan (**NBD-Cl**) using Et_3N as a base, forming the probe **DP-NBD** with high yield in CH_2Cl_2 at room temperature. Moreover, another synthetic route is also investigated. As shown in Scheme 2(B), **NBD-Cl** is treated with piperazine to generate compound **NBD-P**, which is reacted with dansyl chloride to get **DP-NBD** with high yield. All new intermediates and the probe **DP-NBD** are fully characterized by ^1H NMR, ^{13}C NMR and mass spectra.

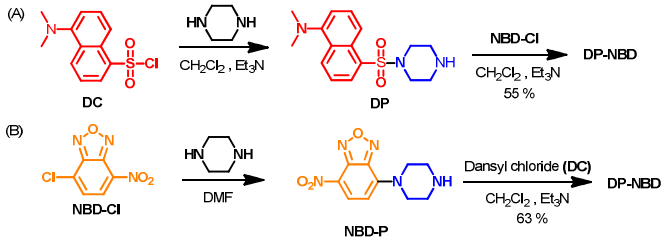

Scheme 2 Two synthetic routes of probe **DP-NBD**

Optical properties

The optical properties of **DP-NBD** are carried out in a buffer solution of HEPES (pH=7.4, 0.02 M) containing 10% DMSO. The solubility of **DP-NBD** in HEPES (pH=7.4, 0.02 M) containing 5% DMSO was 4 μM (Figure S1 in ESI), which was sufficient to stain the cells. Under this condition, **DP-NBD** exhibited absorption maxima (λ_{abs}) at 345 nm (ε =1.20 × 10^4 M^{-1} cm^{-1}), 486 nm (ε = 1.50 × 10^4 M^{-1} cm^{-1}) and emission maxima (λ_{em}) at 545 nm with quantum yield of 0.0021 (ESI in Table S1). Subsequent studies focus on the response of **DP-NBD** (10 μM) towards various guests (10 equiv.) such as (Cys, HCy, GSH, Ala, Tyr, Lys, Glu, Ser, His, Arg, Met, Gly, HSO_3^-, $S_2O_3^{2-}$, SO_3^{2-}, F^-, Cl^-, Br^-, I^-, HPO_4^-, HSO_4^-, NO_3^-, ClO_4^-, OAc^-, CN^-, NO_2^- and H_2S). The UV/Vis absorption response of **DP-NBD** towards various guests is presented in Figure 2A. Only the addition of H_2S to the solution of **DP-NBD** leads to an obvious red-shift of the second absorption peak. Accordingly, the real optical image shows the color of the solution changes from colorless to pink after H_2S is introduced, while other anions and amino acids display few changes, as shown in Figure 2B. The result suggests this probe has good water-solubility, and the UV/Vis absorption spectra strongly indicates that **DP-NBD** can be used as a colorimetric chemosensor for detecting H_2S in aqueous solution.

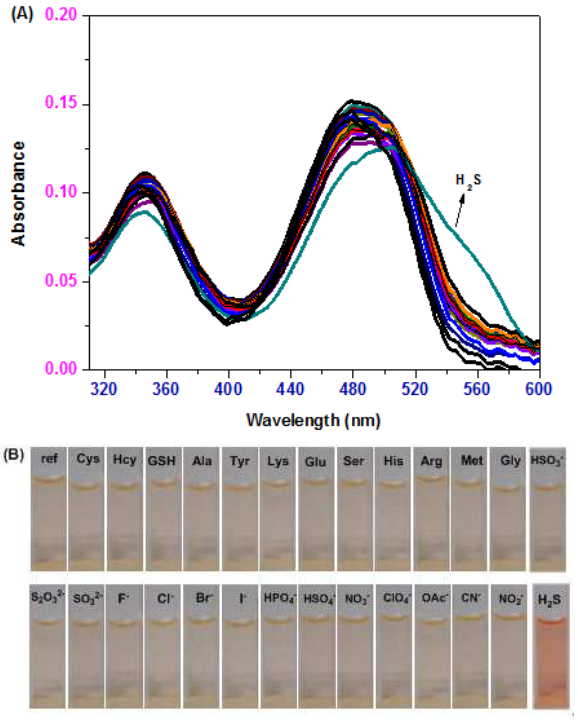

Figure 2 (A) Absorption spectra of **DP-NBD** (10 μM) in the presence of different anions (10 equiv) such as Cys, Hcy, GSH, Ala, Tyr, Lys, Glu, Ser, His, Arg, Met, Gly, HSO_3^-, $S_2O_3^{2-}$, SO_3^{2-}, F^-, Cl^-, Br^-, I^-, HPO_4^-, HSO_4^-, NO_3^-, ClO_4^-, OAc^-, CN^-, NO_2^-, H_2S in a mixed solution of DMSO-HEPES(v/v=10:90, *p*H=7.4, 0.02 M); (B) Absorbance changes of **DP-NBD**. Left to right: **DP-NBD** only (ref), Cys, Hcy, GSH , Ala, Tyr, Lys, Glu, Ser, His, Arg, Met, Gly, HSO_3^-, $S_2O_3^{2-}$, SO_3^{2-}, F^-, Cl^-, Br^-, I^-, HPO_4^-, HSO_4^-, NO_3^-, ClO_4^-, OAc^-, CN^-, NO_2^- and H_2S.

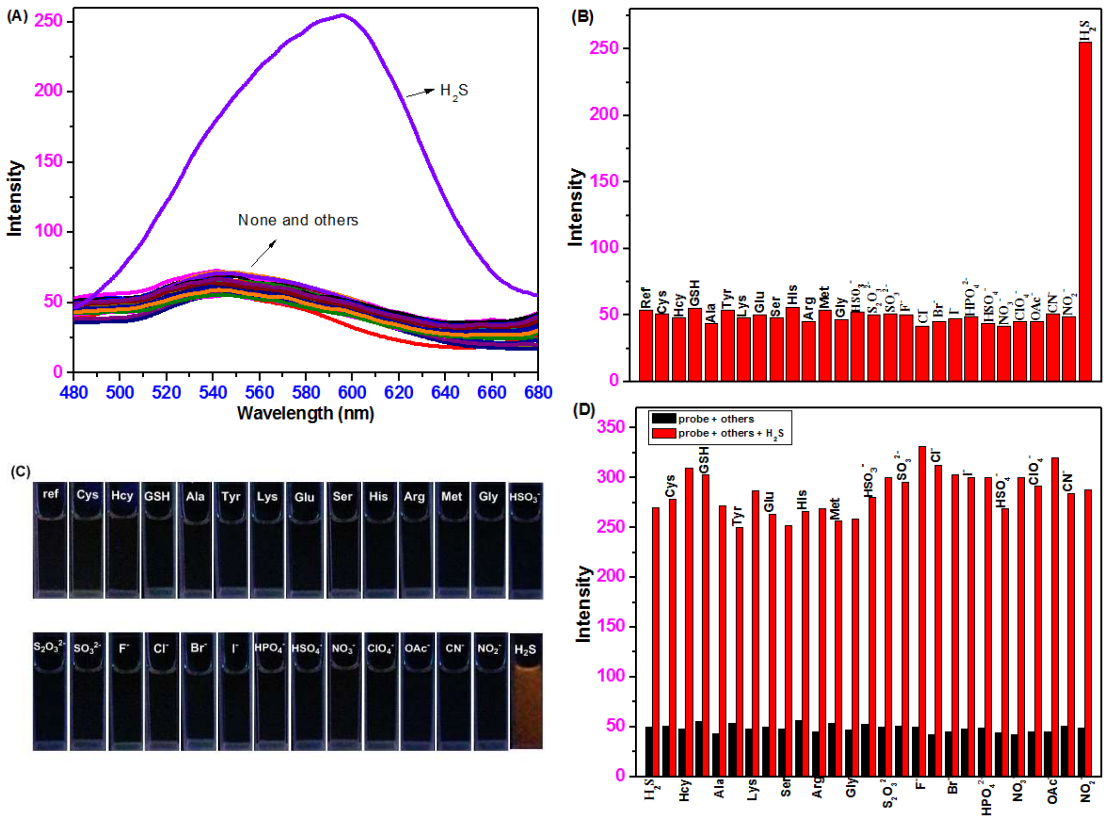

Figure 3 (A) Fluorescence spectra and (B) fluorescence intensity at 595 nm of **DP-NBD** (10 μM) in the presence of different anions (10 equiv.) such as Cys, Hcy, GSH, Ala, Tyr, Lys, Glu, Ser, His, Arg, Met, Gly, HSO_3^-, $S_2O_3^{2-}$, SO_3^{2-}, F^-, Cl^-, Br^-, I^-, HPO_4^-, HSO_4^-, NO_3^-, ClO_4^-, OAc^-, CN^-, NO_2^-, H_2S in a mixed solution of DMSO-HEPES (v/v=10:90, pH=7.4, 0.02 M); (C) Fluorescence changes of **DP-NBD**. Left to right: **DP-NBD** only (ref.), Cys, Hcy, GSH, Ala, Tyr, Lys, Glu, Ser, His, Arg, Met, Gly, HSO_3^-, $S_2O_3^{2-}$, SO_3^{2-}, F^-, Cl^-, Br^-, I^-, HPO_4^-, HSO_4^-, NO_3^-, ClO_4^-, OAc^-, CN^-, NO_2^- and H_2S. (D) Fluorescence response of **DP-NBD** (10 μM). Black bar: **DP-NBD** + other guests. Red bar: **DP-NBD** + other guests + H_2S. (λ_{ex} = 365 nm, λ_{em} = 595 nm, slit: 10/10 nm.)

Next, we investigate the fluorescence behavior of **DP-NBD** towards the guests described above. The fluorescent responses to various tested guests in a buffer solution of HEPES (pH=7.4, 0.02 M) containing 10% DMSO are exhibited in Figure 3A. Similarly, upon the addition of H_2S, a demonstrable red-shift of the emission peak from 545 nm to 594 nm is observed with an around 5-fold enhancement of the fluorescent intensity under the same condition, whereas no significant response is detected when other guest is added (Figure 3B). As a result, an obvious fluorescent change from "off" to "on" can be observed in Figure 3C. Investigation on the interference from other species suggests **DP-NBD** has high selectivity for H_2S, as shown in Figure 3D. The results of an experiment probing the time dependent fluorescence response of **DP-NBD** (10 μM) to H_2S (100 μM) show that the intensity of the 595 nm increases with time, reaching a maximum intensity in 2 h, as well as UV/Vis absorption. This process followed pseudo-first-order kinetics with $k_{obs} = 3.25 \times 10^{-4}$ s^{-1} for the reaction between DP-NBD and H_2S (Figure S2 in ESI). Comparatively, other thiol-based amino acids such as GSH, Cys and Hcy, do not promote as rapid and obvious a fluorescence response of probe **DP-NBD**.[12]

The fluorescent titration experiment of probe **DP-NBD** (10 μM) is investigated upon addition of H_2S (0-30 equiv.) in a buffer solution of HEPES (pH=7.4, 0.02 M) containing 10% DMSO. A significant fluorescence enhancement appears as the amount of H_2S increases, and the fluorescence peak intensity changes of **DP-NBD** correlated well with the concentration of H_2S (Figure S3 in ESI). The sensitivity of **DP-NBD** for H_2S can be calculated on the basis of the linear relationships between the maximum emission intensity at 595 nm and the concentration of H_2S. The probe has a detection limit of 7×10^{-8} M, based on 3σ/K, where σ is the standard deviation of the blank measurements, and K is the slope of the intensity versus the sample concentration plot. The results imply that **DP-NBD** has high sensitivity for H_2S and can be used to detect low levels of H_2S qualitatively.

Bioimaging in living cells

As described above, **DP-NBD** exhibits good water solubility, high selectivity, low detection limit towards H_2S without interferences from other guests. Furthermore fluorescent spectrum at physiological condition (Figure S4 in ESI) and low cytotoxicity (Figure S5 in ESI) authorizes its further application in living cells. HeLa cells are cultured in DMEM medium supplemented with 10% heat-inactivated fetal bovine serum, 100 U/mL penicillin, and 100 U/mL streptomycin and are maintained in an incubator at 37 °C with a 5% CO_2/air environment. **DP-NBD** is incubated with HeLa cells for 30 min at 37 °C, and then the HeLa cells are washed with PBS. The

fluorescent change of the cells is monitored by laser confocal fluorescence microscopy (LCFM). As illustrated by the LCFM images and bright field images (in Figure 4), a red fluorescence image is detected when H_2S is added to the HeLa cells stained by **DP-NBD** and incubated for 1 h. The results suggest that **DP-NBD** is capable of permeating into cells and visualize H_2S. Furthermore, an increasing red fluorescence can be observed when HeLa cells stained by **DP-NBD** are incubated with H_2S for 2 h in Figure 4(H). The results further indicate that probe **DP-NBD** has excellent cell permeability and bio-compatibility.

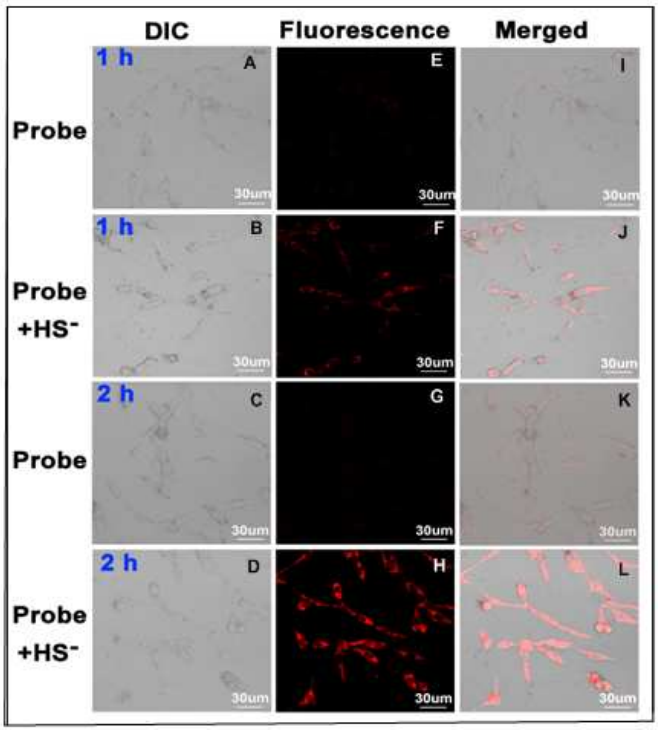

Figure 4 LCFM images of probe **DP-NBD** in HeLa cells. (A-D) bright-field images; (E, G) HeLa cells were treated with **DP-NBD** for 30 min; (F, H) HeLa cells were pre-incubated with **DP-NBD** for 30 min and then treated with H_2S for 1 h or 2h; (I-l) merged images of bright-field and fluorescent image. (λ_{ex} = 365 nm, λ_{em} = 595 nm)

Reaction mechanism

Subsequent efforts is paid on the sensing mechanism of **DP-NBD** with H_2S by MOLDI-TOF mass spectrometry. According to the mass spectrum, a new peak at 320.14 (m/z) corresponding to **DP** can be found when 10 equivalents of H_2S is added into the solution containing **DP-NBD** (Figure S6 in ESI). The result confirms that H_2S cleaves the C-N bond of **DP-NBD** to form the cleavage product **DP**, as described in Scheme 1. Further proof is provided by investigating the fluorescence spectra of fragments **NBD-P** and **DP**. For **NBD-P**, the addition of H_2S leads to the decrease of fluorescent intensity at 545 nm. In comparison to **NBD-P**, **DP** displays a strong emission at 595 nm and no obvious change is observed upon the addition of H_2S. This result further confirms the cleavage product is **DP**.

Consequently, a more detailed analysis of the structure and electron density is performed in an attempt to gain insight into its recognition mechanism. Accordingly, the time-dependent density functional theory (TD-DFT) calculations are used to optimize the structures of **DP-NBD**, **DP** and **NBD-P** at the B3LYP/6-31G* level using a suite of Gaussian 09 programs. The results of the calculations show that the piperazine ring of **DP-NBD** presents a classic chair conformation while the **DP** displays a twist-boat conformation, as shown in Figure 5. For their frontier molecular orbital profiles, the electron density of **DP-NBD** mainly focuses on the dansyl unit in its HOMO orbital while its LUMO orbital lies in the NBD unit. For **DP**, its HOMO and LUMO orbitals almost focus on the dansyl moiety. The HOMO orbital of intermediate **NBD-P** is delocalized piperazine unit by extension to NBD unit while its LUMO is more delocalized in NBD unit. Accordingly, we guess that the **NBD-P** unit possibly plays a role of the PET quencher owing to that the LUMO of **DP** is higher energy then the LUMO of **NBD-P**. As a consequence, the lower LUMO orbital of **NBD-P** can accept an electron from the higher LUMO orbital of **DP**. Upon the treatment of H_2S, the PET process is broken while the DP displays turn-on fluorescence, which is well in agreement with experimental results.

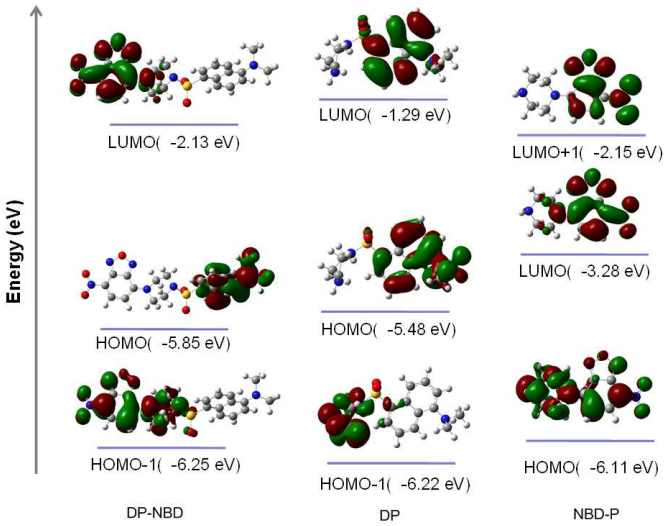

Figure 5 Frontier molecular orbital profiles of molecules based on TDDFT (B3LYP/6-31G*) calculations.

Conclusion

In conclusion, we provide an ideal strategy for designing the turn-on fluorescent probes. In which, a fluorescent compound is selected as a cleavage product to construct the H_2S-responsive probe based on the nucleophilic substituted reaction. According to this strategy, we design and synthesize a H_2S-responsive fluorescent probe which can efficiently detect H_2S with high selectivity and low detection limitation. And the probe shows good water solubility, cell permeability and bio-compatibility. The bioimaging in living cells indicates that this probe can monitor H_2S at cell level. Considering the efficiency and practicability of this strategy, we believe it will be commonly used to design the turn-on fluorescent probe in near future. Furthermore, the small molecular H_2S probe can be used as an efficient tool to investigate the biological functions that are related to H_2S.

Experimental Section

Materials and instrumentation. All manipulations were carried out under an argon atmosphere using standard Schlenk techniques, unless otherwise stated. All commercials were used

as received without further purification. ^{1}H and ^{13}C spectra were collected on Bruker 400 MHz spectrometer (Bruker, Bremen, Germany) in DMSO-d_6 and $CDCl_3$ with Me_4Si as an internal reference. UV–Vis spectra were obtained using Hitachi U-3310 visible recording spectrophotometer. Fluorescence spectra were obtained using Perkin Elmer LS-55. Mass spectra were measured in the ESI mode. The theoretical calculations were performed at the B3LYP/6-31G* level by using the Gaussian 09 suite of programs.

Synthesis of DP. To a 25 mL round-bottomed flask was added 134.8 mg (0.5 mmol) of dansyl chloride and 172.2 mg (2 mmol) of piperazine. Then CH_2Cl_2 and Et_3N were added. The reaction was stirred at room temperature for 4 h. The mixture was then evaporated and the residue was purified with column chromatography (silica gel, dichloromethane/methanol = 30:1, v/v). A yellow green solid (154 mg) was obtained, yield: 96%. ^{1}H NMR (400 MHz, DMSO-d_6): δ8.54-8.52 (d, J = 8.00 Hz, 1H), 8.35-8.32 (d, J = 12.00 Hz, 1H), 8.12-8.10 (d, J = 8.00 Hz,1H), 7.69-7.66 (t, J = 8.00 Hz, 1H), 7.63-7.59 (t, J = 8.00 Hz, 1H), 7.28-7.26 (d, J = 8.00 Hz, 1H), 2.95 (s, 4H), 2.84 (s, 6H), 2.65 (s, 4H). EI-MS m/z (M^+) calcd 319.13, found 319.11.

Synthesis of NBD-P. To a 25 mL round-bottomed flask was added 199.5 mg (0.5 mmol) of 4-Chloro-7-nitrobenzo-2,1,3-oxadiazole and 172.2 mg (2 mmol) of piperazine. Then DMF was added. The reaction was stirred for 4 h at 85 °C. The mixture was then evaporated and the residue was purified with column chromatography (silica gel, dichloromethane / ethyl acetate = 6:1, v/v). A red solid (97.6 mg) was obtained, yield: 78%. ^{1}H NMR (400 MHz, DMSO-d_6): δ8.47-8.45 (d, J = 8.00 Hz, 1H), 6.66-6.64 (d, J = 8.00 Hz, 1H), 4.08 (s, 4H), 2.95-2.93 (t, J = 4.00 Hz, 4H). EI-MS m/z (M^+) calcd 249.08, found 249.02.

Synthesis of DP-NBD. To a 25 mL round-bottomed flask was added 95.7 mg (0.3 mmol) of **DP** and 5 mL of CH_2Cl_2. Then 65.8 mg (0.33 mmol) of 4-Chloro-7-nitrobenzo-2,1,3-oxadiazole was added. The reaction was stirred at room temperature for 12 h. The mixture was then evaporated and the residue was purified with column chromatography (silica gel, dichloromethane). A orange solid (80.0 mg) was obtained, yield: 55%. ^{1}H NMR (400 MHz, DMSO-d_6): δ8.20-8.18 (d, J = 8.00 Hz, 1H), 8.13-8.10 (d, J = 12.00 Hz, 1H), 8.00-7.98 (d, J = 8.00 Hz, 1H), 7.86-7.84 (d, J = 8.00 Hz, 1H), 7.37-7.33 (t, J = 8.00 Hz, 1H), 7.32-7.28 (t, J = 8.00 Hz, 1H), 6.94-6.92 (d, J = 8.00 Hz, 1H), 6.26-6.24 (d, J = 8.00 Hz, 1H), 3.85-3.83 (t, J = 4.00 Hz, 4H), 3.10-3.08 (t, J = 4.00 Hz, 4H),2.19 (s, 6H) ^{13}C NMR ($CDCl_3$, 400 MHz): 146.86, 139.58, 139.33, 129.26, 126.98, 126.12, 125.72, 125.11, 124.99, 123.23, 119.89, 117.95, 113.91, 110.26, 98.20, 43.71, 40.16, 39.87, 24.47. EI-MS m/z (M^+) calcd 482.11, found 482.33.

Optical studies. Stock solutions of **DP-NBD** (1 mM) was prepared in HPLC grade DMSO. Stock solutions of analytes (10 mM) were prepared in HEPES buffer solution (pH=7.4, 0.02 M). The stock solutions of analytes were diluted to desired concentrations with HEPES buffer solution when needed. For a typical optical measurements, **DP-NBD** was diluted to 10 μM in a DMSO-HEPES buffer solution (v/v=10:90, pH=7.4, 0.02 M), and 3.0 mL of the resulting solution was placed in a quartz cell. The UV–Vis or fluorescent spectra were then recorded upon addition of analytes at 25 °C. Emission spectra of the sensor in the presence of various guests (Cys, Hcy, GSH, Ala, Tyr, Lys, Glu, Ser, His, Arg, Met, Gly, HSO_3^-, $S_2O_3^{2-}$, SO_3^{2-}, F^-, Cl^-, Br^-, I^-, HPO_4^-, HSO_4^-, NO_3^-, ClO_4^-, OAc^-, CN^-, NO_2^-, H_2S) were measured by excitation with 365 nm. The slit size for excitation and emission was 10 × 10, respectively.

Cell culture and imaging. The human cervical carcinoma cell lines HeLa were obtained from American Type Culture Collection (ATCC, USA). The cell lines were cultured in DMEM medium supplemented with 10% (v/v) calf serum, penicillin (100 U mL/1) and (100 mg mL/1) streptomycin. Cells were maintained at 37 °C in a humidified atmosphere containing 5% CO_2.

The cells were seeded in each well of 96-well plates at a density of 5 × 10^5 cells/well and subsequently incubated for 24 h in CO_2 culture box. The cells were further maintained at 37 °C for 24 h after treatment of the probe DP-NBD at a wide concentration range from 1μM to 100 μM. Each well was washed three times with PBS (pH = 7.0) before addition of MTT solution (15 mL, 5.0 mg mL^{-1}) and the cells were incubated for another 4 h. The medium containing MTT was then carefully removed and 150 μL of DMSO was added into each well. The plates were gently shaken for 15 min at room temperature before the absorbance measurement. Six independent experiments were carried out for *in vitro* cytotoxicity assay. All the samples were assayed in quadruplicate and the cell viability was calculated using the following formula: cell viability = (mean absorbance of test wells - mean absorbance of medium control wells)/(mean absorbance of untreated wells - mean absorbance of medium control well) × 100%.

The cells were seeded in laser confocal fluorescence microscope (LCFM) culture dishes with a density of 5 × 10^5 cells/well. The cell lines were cultured in DMEM medium supplemented with 10% (v/v) calf serum, penicillin (100 UmL-1) and streptomycin (100 mg mL^{-1}). Cells were maintained at 37 °C in a humidified atmosphere containing 5% CO_2. When the whole cells took up 70%-80% space of culture dishes, two groups were studied as followed. The cells were further maintained at 37 °C for 0.5 h after treatment of the **DP-NBD** (100 μL, 10 μg/mL) and the medium was then carefully removed and each dish was washed three times with PBS (pH=7.0). Then the cells were treated with NaHS (100 μL, 1 mg/mL) for 1 h or 2 h. And the medium was then carefully removed and each dish was washed three times with PBS (pH=7.0). Then the fluorescence of **DP-NBD** was collected by LCFM (FV 1000, Olympus, Japan).

DFT calculation. Accordingly, density functional theory (DFT) calculations were used to optimize the structures of **DP-NBD**, **DP** and **NBD-P** at the B3LYP/6-31G* level using a suite of Gaussian 09 programs.

Acknowledgements

The authors acknowledge financial support from National Natural Science Foundation of China (21272088, 21472059, 21402057 and 81371684), the Scientific Research Foundation for the Returned Overseas Chinese Scholars, Ministry of Education and the self-determined research funds of CCNU from the colleges' basic research and operation of MOE (CCNU14A05009, CCNU14F01003).

Notes and references

[a] Key Laboratory of Pesticide and Chemical Biology of the Ministry of Education, College of Chemistry, Central China Normal University, Wuhan 430079, P. R. China. E-mail: yinj@mail.ccnu.edu.cn

[b] Department of Biomedical Engineering, School of Engineering, China Pharmaceutical University, 24 Tongjia Lane, Gulou District, Nanjing 210009, China. E-mail: chenhaiyan@cpu.edu.cn
[c] State Key Laboratory of Materials-Oriented Chemical Engineering, College of Chemistry and Chemical Engineering, Nanjing Tech University, Nanjing 210009, China.
[1]They contributed equally to this work.
†Electronic Supplementary Information (ESI) available: The ^{1}H NMR, ^{13}C NMR and MS spectra, UV/vis absorption and fluorescence spectra. See DOI: 10.1039/c000000x/

1 (a) A. Kazuho and H. J. Kimura, *Neurosci.*, 1996, **16**, 1066-1071; (b) R. Wang, *Antioxid. Redox. Signal.*, 2003, **5**, 493-501; (c) H. Kimura, Y. Nagai, K. Umemura and Y. Kimura, *Antioxid. Redox. Signal.*, 2005, **7**, 795-803; (d) J. M. Ritter, *Br. J. Clin. Pharmacol.*, 2010, **69**, 573-575; (e) R.Wang, *Physiol. Rev.*, 2012, **92**, 791-896; (e) H. Peng, Y. Cheng, C. Dai, A. L. King, B. L. Predmore, D. J. Lefer and B. Wang, *Angew. Chem. Int. Ed.* 2011, **50**, 9672-9675.
2 (a) L. F. Hu, M. Lu, P. T. Hon Wong and J. S. Bian, *Antioxid. Redox. Signal.*, 2011, **15**, 405-419; (b) A. Martelli, L. Testai, M. C. Breschi, C. Blandizzi, A. Virdis, S. Taddei and V. Calderone, *Med. Res. Rev.*, 2012, **32**, 1093-1130; (c) C. Szabo, *Antioxid. Redox. Signal.*, 2012, **17**, 68-80; (d) N. R. Prabhakar, *Respir. Physiol. Neurobiol.*, 2012, **184**, 165-169; (e) B. S. King, *Free Radic. Biol. Med.*, 2013, **55**, 21-26.
3 (a) M. H. Stipanuk and P. W. Beck, *Biochem. J.*, 1982, **206**, 267-277; (b) H. Kimura, *Mol. Neurobiol.*, 2002, **26**, 13-19; (c) K. H. Jhee and W. D. Kruger, *Antioxid. Redox. Signal*., 2005, **7**, 813-822; (d) N. Shibuya, M. Tanaka, M. Yoshida, Y. Ogasawara, T. Togawa, K. Ishii and H. Kimura, *Antioxid. Redox. Signal.*, 2009, **11**, 703-714; (e) B. D. Paul and S. H. Snyder, *Nat. Rev. Mol. Cell Biol.*, 2012, **13**, 499-507.
4 R. J. Reiffenstein, W. C. Hulbert and S. H. Roth, *Annu. Rev. Pharmacol. Toxicol.*, 1992, **32**, 109-134.
5 (a) J. Radford-Knoery and G. A. Cutter, *Anal. Chem.*, 1993, **65**, 976-982; (b) M. M. F. Choi, *Analyst*, 1998, **123**, 1631-1634; (c) N. S. Lawrence, J. Davis, L. Jiang, T. G. J. Jones, S. N. Davies and R. G. Compton, *Electroanalysis*, 2000, **18**, 1453-1460; (d) B. Spilker, J. Randhahn, H. Grabow, H. Beikirch and P. Jeroschewski, *J. Electroanal. Chem.*, 2008, **612**, 121-130; (e) M. G. Choi, S. Cha, H. Lee, H. L. Jeon and S. K. Chang, *Chem. Commun.*, 2009, **45**, 7390-7392; (f) M. Ishigami, K. Hiraki, K. Umemura, Y. Ogasawara, K. Ishii and H. Kimura, *Antioxid. Redox. Signal.*, 2009, **11**, 205-214.
6 For selected reviews, see: (a) H. J. Peng, W. X. Chen, S. Burroughs, and B. H. Wang，*Curr. Org. Chem.*, 2013, **17**, 641-653; (b) F. B. Yu, X. Y. Han and L. X. Chen，*Chem. Commun.*, 2014, **50**, 12234-12249; (c) Y. Zhao, T. D. Biggs and M. Xian, *Chem. Commun.*, 2014, **50**, 11788-11805; (d) V. S. Lin, W. Chen, M. Xian and C. J. Chang, *Chem. Soc. Rev.*, 2015, DOI: 10.1039/C4CS00298A; (e) V. S. Lin and C. J. Chang, *Curr. Opin. Chem. Biol.*, 2012, **16**, 595-601; (f) T. Y. Liu, Z. C. Xu , D. R. Spring and J. N. Cui, *Org. Lett.*, 2013, **15**, 2310–2313; (g) B. Peng and M. Xian, *Asian J. Org. Chem.*, 2014, **3**, 914-924; (h) A.R. Lippert, *J. Inorg. Biochem.*, 2014, **133**, 136-142; (i) J. F. Li, C. X. Yin and F. J. Huo, *RSC Adv.*, 2015, **5**, 2191-2206; (j) Z. Guo, G. Q, Chen, G. M. Zeng, Z. W. Li, A.-W. Chen, J. J. Wang and L. B. Jiang, *Analyst*, 2015, **140**, 1772–1786.
7 For selected literatures, see: (a)A. R. Lippert, E. J. New and C. J. Chang, *J. Am. Chem. Soc.*, 2011, **133**, 10078-10080; (b) F. Yu, P. Li, G. Li, G. Zhao, T. Chu and K. Han, *J. Am. Chem. Soc.*, 2011, **133**, 11030-11033; (c) X. Cao, W. Lin and L. He, *Org. Lett.*, 2011, **13**, 4716-4719; (d) K. Sasakura, K. Hanaoka, N. Shibuya, Y. Mikami, Y. Kimura, T. Komatsu, T. Ueno, T. Terai, H. Kimura and T. Nagano, *J. Am. Chem. Soc.*, 2011, **133**, 18003-18005; (e) L. A. Montoya and M. D. Pluth, *Chem. Commun.*, 2012, **48**, 4767-4769; (f) M. Wu, K. Li, J Hou, Z. Huang and X. Yu, *Org. Biomol. Chem.*, 2012, **10**, 8342-8347; (g) Y. Qian, L. Zhang, S. Ding, X. Deng, C. He, X. E. Zheng, H.-L. Zhu and J. Zhao, *Chem. Sci.*, 2012, **3**, 2920-2923; (h) X. Cao, W. Lin, K. Zheng and L. He, *Chem. Commun.*, 2012, **48**, 10529-10531; (i) J. Zhang, Y. Q. Sun, J. Liu, Y. Shi and W. Guo, *Chem. Commun.*, 2013, **49**, 11305-11307; (j) C. Wei, Q. Zhu, W. Liu, W. Chen, Z. Xi and L. Yi, *Org. Biomol. Chem.*, 2014, **12**, 479-485.
8 (a) D. T. Quang and J. S. Kim, *Chem. Rev.*, 2010, **110**, 6280–6301; (b) Y. M. Yang, Q. Zhao, W. Feng and F. Y. Li, *Chem. Rev.*, 2013, **113**, 192-270. (c) M. j Cao, L-N Jiang, F. Hu, Y. F. Zhang, W. C. Yang, S. H. Liu and J. Yin, *RSC Adv.*, 2015, **5**, 23666-23670.
9 For selected, see: (a) Y. Qian, J. Karpus, O. Kabil, S. Y. Zhang, H. L. Zhu, R. Banerjee, J. Zhao and C. He, *Nat. Commun.*, 2011, **2**, 495; (b) Z. Xu, L. Xu, J. Zhou, Y. Xu, W. Zhu and X. Qian, *Chem. Commun.*, 2012, **48**, 10871-10873; (c) X. Cao, W. Lin, K. Zheng and L. He, *Chem. Commun.*, 2012, **48**, 10529–10531; (d) X. Li, S. Zhang, J. Cao, N. Xie, T. Liu, B. Yang, Q. He and Y. Hu, *Chem. Commun.*, 2013, **49**, 8656-8658; (e) T. Liu, X. Zhang, Q. Qiao, C. Zou, L. Feng, J. Cui and Z. Xu, *Dyes Pigm.*, 2013, **99**, 537–542; (f) Y. Liu and G. Feng, *Org. Biomol. Chem.*, 2014, **12**, 438–445.
10 For selected, see: (a) C. Liu, J. Pan, S. Li, Y. Zhao, L. Y. Wu, C. E. Berkman, A. R. Whorton and M. Xian, *Angew. Chem., Int. Ed.*, 2011, **50**, 10327-10329; (b) C. Liu, B. Peng, S. Li, C.-M. Park, A. R. Whorton and M. Xian, *Org. Lett.*, 2012, **14**, 2184-2187; (c) X. Wang, J. Sun, W. Zhang, X. Ma, J. Lv and B. Tang, *Chem. Sci.*, 2013, **4**, 2551-2556; (d) C. Wei, L. Wei, Z. Xi and L. Yi, *Tetra. Lett.*, 2013, **54**, 6937–6939. (e) Y. Chen, C. Zhu, Z. Yang, J. Chen, Y. He, Y. Jiao, W. He, L. Qiu, J. Cen and Z. Guo, *Angew. Chem., Int. Ed.*, 2013, **125**, 1732–1735; (f) C. Y. Zhang, L. Wei, C. Wei, J. Zhang, R. Y. Wang, Z. Xi and L.Yi, *Chem. Commun.*, 2015, **51**, 7505—7508. (g) B. Roubinet, L. Bailly, E. Petit, P-Y. Renard and A. Romieu, *Tetrahedron Lett.*, 2015, **56**, 1015–1019.
11 J. Yin, Y. Kwon, D. Kim, D. Lee, G. Kim, Y. Hu, J. H. Ryu and J. Yoon, *J. Am. Chem. Soc.*, 2014, **136**, 5351-5358.
12 D. Lee, G. Kim, J. Yin and J. Yoon, *Chem. Commun.,* 2015, **51**, 6518-6520.

Journal Name

RSCPublishing

ARTICLE

A Fluorescent Turn-on H_2S-responsive Probe: Design, Synthesis and Application

Yufeng Zhang,[1a] Haiyan Chen,[1b*] Dan Chen,[b] Di Wu,[a] Xiaoqiang Chen,[c] Sheng Hua Liu*[a] and Jun Yin*[a]